Journal of Organometallic Chemistry, 181 (1979) 131—141

SINGLE-CRYSTAL RAMAN STUDY OF DIRHENIUM DECACARBONYL *

DAVID M. ADAMS and MARTIN A. HOOPER **

Department of Chemistry, University of Leicester, Leicester LE1 7RH (Great Britain)

(Received February 26th, 1979)

Summary

A single-crystal Raman study of $Re_2(CO)_{10}$ is reported from which 20 of the 21 Raman-active modes of this D_{4d} molecule have been assigned. All six lattice modes were identified below 70 cm^{-1}. In respect of the long-disputed assignment of ν(Re—Re), for which two possibilities exist (107 and 129 cm^{-1}), the balance of the new evidence is in favour of the lower band. Comparisons are drawn with assignments for $Mn_2(CO)_{10}$ and $Re(CO)_5X$, (X = halogen), respectively and anomalies noted.

The first infrared spectra of $Mn_2(CO)_{10}$ and $Re_2(CO)_{10}$ were published in 1954 [1]. A quarter of a century later, following several studies [2] of both materials, their far-IR spectra remain inadequately determined and assigned. Indeed no further IR work on either decacarbonyl has been reported since 1971, other than studies of the ν(CO) region [3,5]. A better situation pertains in respect of their Raman spectra. Single-crystal data for $Mn_2(CO)_{10}$ led to a rather complete assignment of the entire spectrum [2], and preliminary single-crystal ν(CO) data were also obtained for $Re_2(CO)_{10}$ [6]. Subsequently reports have appeared dealing with aspects of the ν(CO) region [7] and of metal—metal stretching frequencies [8—10], but no further attempts have been made at a complete determination and assignment of the Raman spectrum of $Re_2(CO)_{10}$. We now report the results of a single-crystal Raman investigation of $Re_2(CO)_{10}$.

In interpreting the spectra of either decacarbonyl it is helpful to consider these molecules as two coupled C_{4v} $M(CO)_5$ moieties, and to ensure that the assignments are consistent with those for the somewhat simpler $M(CO)_5X$ systems, where X = H, Cl, Br or I. The ν(CO) region of the spectra of these

---

* Dedicated to Joseph Chatt on his 65th birthday, David M. Adams was a member of Joseph Chatt's research group in I.C.I. at "The Frythe", Welwyn for four years from November 1958, with responsibility for infrared and far-infrared spectroscopy.

** Present address: Applied Science Department, Gippsland Institute of Advanced Education, Churchill, Victoria 3842 (Australia).

materials has been studied extensively, but in respect of the region below 800 cm^{-1}, in which all modes other than ν(CO) lie, the assignment for $Mn(CO)_5Br$ is the only one that can be regarded as settled with any degree of confidence [11,12]. Several studies have been made of the low-frequency IR and Raman spectra of the manganese series [13—20], and rather fewer of the rhenium analogues [15,16,18,21,22]. Of these, only Clark and Crosse [16] investigated all six halogeno complexes and used cooled samples for far-IR study. From these collected data, probable assignments can be advanced for the δ(MCO), ν(M—CO) regions (300—800 cm^{-1}) of all the halogeno complexes by reference to the definitive work [11] on $Mn(CO)_5Br$, but understanding of the region below 150 cm^{-1}, which contains all δ(CMC) deformations and the lattice modes, is in a most unsatisfactory state in respect of both data and assignments.

Theory

$Mn_2(CO)_{10}$ and $Re_2(CO)_{10}$ are isomorphous, crystallising with the symmetry of the monoclinic group $C2/c$, C_{2h}^6 with a bimolecular primitive cell [23,24]. The molecules are on C_2 sites (Wyckoff e) and have approximate D_{4d} symmetry.

TABLE 1

DISTRIBUTION AND NUMBERING OF MODES FOR D_{4d} $M_2(CO)_{10}$

A_1 (Raman-active)		*E_1 (IR-active)*	
ν_1	ν(CO)equatorial	ν_{17}	ν(CO)equatorial
ν_2	ν(CO)axial	ν_{18}	δ(MCO)
ν_3	π(MCO) [a]	ν_{19}	π(MCO)
ν_4	ν(M—CO) [b]	ν_{20}	ρ(MCO) [c] axial
ν_5	ν(M—CO) [b]	ν_{21}	ν(M—CO)equatorial
ν_6	π(CMC) [a]	ν_{22}	δ(CMC)
ν_7	ν(M—M) [e]	ν_{23}	π(CMC)
		ν_{24}	Δ [d]
A_2 (inactive)			
ν_8	δ(MCO) [a]	*E_2 (Raman-active)*	
		ν_{25}	ν(CO)equatorial
B_1 (inactive)		ν_{26}	δ(MCO)
ν_9	δ(MCO)	ν_{27}	π(MCO)
ν_{10}	Torsion	ν_{28}	ν(M—CO)equatorial
		ν_{29}	δ(CMC)
B_2 (IR-active)		ν_{30}	π(CMC)
ν_{11}	ν(CO)equatorial		
ν_{12}	ν(CO)axial	*E_3 (Raman-active)*	
ν_{13}	π(MCO)	ν_{31}	ν(CO)equatorial
ν_{14}	ν(M—CO) [b]	ν_{32}	δ(MCO)
ν_{15}	ν(M—CO) [b]	ν_{33}	π(MCO)
ν_{16}	π(CMC)	ν_{34}	ρ(MCO)axial [c]
		ν_{35}	ν(M—CO)equatorial
		ν_{36}	δ(CMC)
		ν_{37}	π(CMC)
		ν_{38}	Δ [d]

[a] π indicates a deformation out of the plane defined by the four oxygen or carbon atoms of each equatorial set; the transition moment is therefore parallel to the molecular S_8 axis. δ indicates a deformation in these planes. [b] ν(M—CO)axial and ν(M—CO) equatorial are probably mixed in type. [c] An MCO angle deformation of the axial carbonyls. [d] Skeletal deformations involving MMC angles. [e] Modes numbers 7, 10, 24 and 38 may be considered as arising from coupling two C_{4v} $M(CO)_5$ moieties. All other modes of $M_2(CO)_{10}$ arise from coupling of two modes of the same type in $M(CO)_5$, as shown by the correlation of Table 2.

TABLE 2

FACTOR GROUP ANALYSIS AND CORRELATION TABLES FOR $M_2(CO)_{10}$

C_{2h}^6	N_{Total}	T_A [a]	T	R	N_{int}	Activity
A_g	33		1	1	31	x^2, y^2, z^2, xy
B_g	33		2	2	29	yz, zx
A_u	33	1		1	31	IR
B_u	33	2		2	29	IR

[a] T_A = acoustic, T = translatory, R = libratory, N_{int} = molecular internal modes (for two coupled molecules in the primitive unit cell).

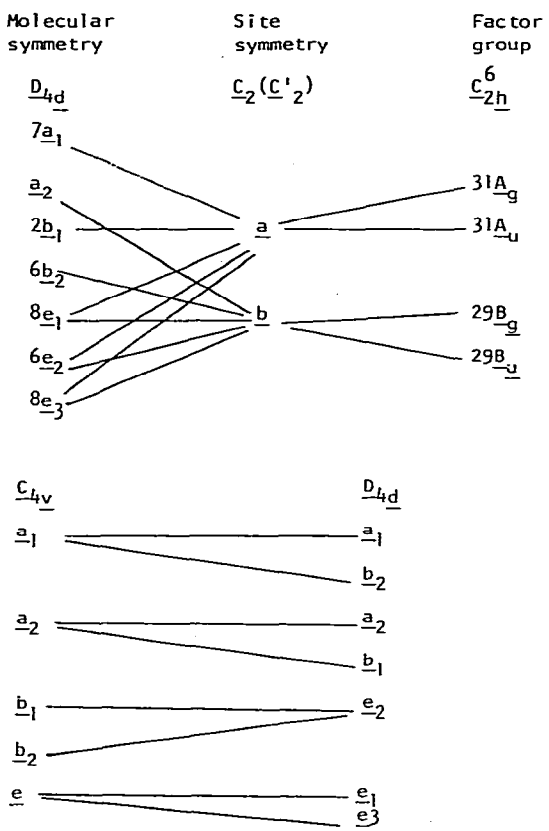

The metal—metal bonds are all parallel to one another and lie in planes perpendicular to the unique axis *b*.

The distribution among symmetry species, and approximate descriptions, of the molecular modes is shown in Table 1. A factor group analysis is shown in Table 2, together with the correlation to C_{4v} for comparison with $M(CO)_5X$ species.

The axial directions used in the single-crystal Raman experiments coincide with the crystallographic axes *a*, *b*, and c^*, where c^* is the third member of an orthogonal set of which *a* and *b* are members. The unique axis *b* is re-labelled *Z* to maintain consistency with the C_{2h} character table, and coincides with

TABLE 3

RAMAN TENSOR ELEMENTS AND ACTIVITIES FOR $Re_2(CO)_{10}$

Experimental axes				
(X, Y, Z)	C_{2h}^6	(X', Y', Z)	D_{4d}(xyz)	
$X(ZZ)Y$	A_g	ZZ	xx	$a_1 + e_2$
$X(YX)Y$	A_g	$X'Y', X'X', Y'Y'$	yy, zz, yz	$a_1 + e_2 + e_3$
$X(ZX)Y$	B_g	$X'Z, Y'Z$	xz, yz	$e_2 + e_3$
$X(YZ)Y$	B_g	$X'Z, Y'Z$	xz, yx	$e_2 + e_3$

one of the optical indicatrix axes; the other two indicatrix axes complete an orthogonal set but their position within the ac^* plane is not fixed by any symmetry requirement and they may show dispersion. These relationships are summarised in Table 3 and illustrated by Fig. 1.

A molecular crystal may be considered, to a first approximation, as an oriented gas. Since the single-crystal Raman experiments are to be conducted in terms of the crystal XYZ axis set of Fig. 1, we need to find how the D_{4d} tensor components relate to them. A clockwise rotation of 42° about the molecular x-axis (coincident with a crystallographic C_2-axis), followed by interchange of molecular x- and z-axis labels, brings the two axis sets into coincidence. The re-orientation of the D_{4d} tensor components is achieved by a similarity transformation, TRT^t, where

$$T = \begin{bmatrix} 1 & 0 & 0 \\ 0 & \cos 42 & \sin 42 \\ 0 & -\sin 42 & \cos 42 \end{bmatrix}$$

and R is, in turn, the a_g, e_2 and e_3 Raman tensors. For a_1 species, $R = ({}^{a}a_{b})$ and hence in terms of crystallographic axes, the re-oriented and re-labelled tensor becomes:

$$\begin{bmatrix} [0.45a + 0.55b] & 0.5(b - a) & 0 \\ 0.5(b - a) & [0.55a + 0.45b] & 0 \\ 0 & 0 & a \end{bmatrix} \approx \begin{bmatrix} b/2 & b/2 & 0 \\ b/2 & b/2 & 0 \\ 0 & 0 & a \end{bmatrix}$$

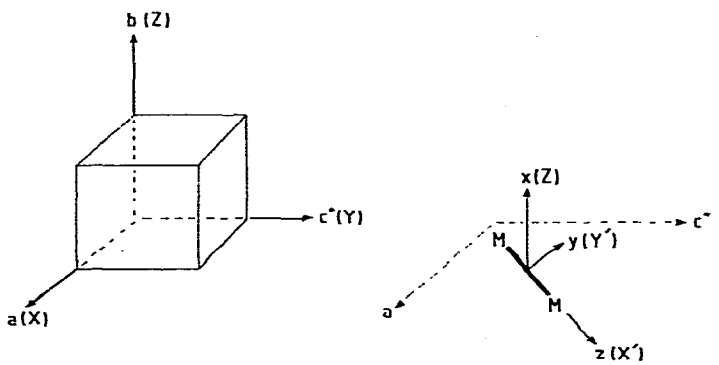

Fig. 1. Relationships between the axes used in this study.

where advantage has been taken of the fact that polarisability along the Re– Re bond is considerably greater than that normal to it. Similarly, we obtain for e_2 and e_3:

$$\begin{bmatrix} -0.45d & 0.50d & 0.67e \\ 0.50d & -0.55d & 0.74e \\ -0.67e & 0.74e & d \end{bmatrix} \quad e_2 \qquad \text{and} \qquad \begin{bmatrix} -f & 0.1f & 0.74f \\ 0.1f & f & 0.67f \\ 0.74f & 0.67f & 0 \end{bmatrix} \quad e_3$$

These results are largely a semi-quantitative restatement of the information conveyed by the correlation of Table 1, but add to them usefully. Thus, we note that e_2 species should appear in (ZZ) experiments whereas e_3 species are characterised by (ideally) zero intensity in (ZZ). The intensity generated by e_3 species in (XZ) should be some 50 times that found by (XY) experiments (since Raman intensity is proportional to the square of the relevant tensor component). The species expected to be active in particular experiments are collected in Table 3.

Experimental

$Re_2(CO)_{10}$ from Alfa Inorganics was resublimed twice in vacuo. Crystals were grown by a further very slow sublimation onto a cold-finger held at ice temperature. Very good quality crystals were obtained of linear dimensions ca. 1 mm. The face development was different from that found for $Mn_2(CO)_{10}$ grown under similar conditions [2]. Axes were located by the X-ray Weissenberg method.

Raman spectra were recorded using a Coderg Ph0 spectrometer with DC detection and an EMI 9558B PM tube at ambient temperature, and excited with ca. 35 mW 632.8 nm radiation at the sample.

Results and discussion

The new data are given in Table 4 and illustrated by Fig. 2 and 3.

ν(CO) region. The assignment of the ν(CO) region of $Mn_2(CO)_{10}$ and $Re_2(CO)_{10}$ was established on the basis of Raman polarisation and IR evidence for solutions [6], and Raman results for oriented single crystals [2]. These papers contained a preliminary account of the ν(CO) part of the work now reported. Subsequently, Bor and Sbrignadello [4] have made a very thorough IR study of these materials, paying particular attention to isotopic data, and have convincingly demonstrated by force constant analyses that the many data show full internal consistency on the basis of the assignment shown in Table 4.

Assignment of ν_1, ν_{11} and ν_{25} is unequivocal; the detailed arguments presented earlier [2] for $Mn_2(CO)_{10}$ apply identically. The only difficulty arises in dealing with the three ν(CO) bands below 2000 cm^{-1}. The lowest is of B_g symmetry and is plainly a component of ν_{31}, e_3, but it remains to determine which A_g component (1986 or 1976 cm^{-1}) belongs to it. The difficulty arises because the ν_2, a_1

TABLE 4

SINGLE-CRYSTAL RAMAN FREQUENCIES AND PEAK HEIGHTS FOR $Re_2(CO)_{10}$

Frequency (cm^{-1})	A_g		B_g		Assignment		
	$X(ZZ)Y$	$X(YX)Y$	$X(ZX)Y$	$X(YZ)Y$	C_{2h}^6	D_{4d}	
2125	65	5	2	1	A_g	a_1 (equatorial)	ν_1
2072	—	—	<<1	—	B_g	b_2	ν_{11}
2025	100	18	5	3	A_g }	e_2	ν_{25}
2016	2	2	60	45	B_g		
1986	3	33	—	1	A_g }	e_3	ν_{31}
1972	1	—	5	5	B_g		
1976	27	95	2	4	A_g	a_1 (axial)	ν_2
613	2	—	—	—	A_g	a_1	ν_3
595	—	<1	—	—	A_g }	e_3	ν_{32}
592	—	—	1	1	B_g		
539	—	—	1	3	B_g }	e_3	ν_{33}
534	3	<1	—	—	A_g		
513	9	—	—	<1	A_g/B_g	e_2	ν_{26}
505	9	1	—	<1	A_g/B_g	e_2	ν_{27}
476	60	8	3	1	A_g	a_1	ν_4
459.5	100	18	4	4	A_g	a_1	ν_5
451	25	5	4	10	A_g/B_g	e_2	ν_{28}
434	2	—	—	—	A_g	e_1	ν_{21}
422	<<1	<1	<<1	<<1	A_g/B_g	e_1	
394	—	10	—	—	A_g }	e_3	ν_{35}
389	1	2	11	38	B_g		
135	95	15			A_g }	e_2	ν_{29}
133				20	B_g		
129	95				A_g	a_1	ν_6
122		100			A_g }	e_3	ν_{36}
119			40	75	B_g		
107	28	42			A_g	a_1	ν_7
100		12	60	10	A_g/B_g	e_3	ν_{37}
95				30	B_g	b_2 or e_1	
85				50	B_g }	e_2	ν_{30}
81	10	27			A_g		
71			33		B_g	$\nu_L(R_z)$	
65	<1	5	33	36	A_g/B_g	e_3	ν_{38}
41			25	73	B_g	$\nu_L(R_{x,y})$	
33	19	42			A_g	$\nu_L(R_{x,y})$	
30			70	175	B_g }	translatory	
23			12		B_g }	lattice modes	
18		28			A_g }		

and ν_{31}, e_3 bands are closer together in $Re_2(CO)_{10}$ (9.0 cm^{-1}) than in $Mn_2(CO)_{10}$ (16.0 cm^{-1}), taking solution values.

There are three arguments in favour of linking ν_2, a_1 with the crystal band at 1976 cm^{-1}. Firstly the high (ZZ) intensity of the 1986 cm^{-1} band is incompatible with an e_3 origin, which should (ideally) have zero intensity in this tensor component. Secondly, this assignment accounts for the differing intensity patterns exhibited by powder samples of $Mn_2(CO)_{10}$ and $Re_2(CO)_{10}$ in this region (Fig. 1 and 2 of ref. 2). Thirdly, if the 1976 cm^{-1} band were a component of ν_{31}, e_3, the site splitting would be uniquely small for these compounds (4 cm^{-1}), whereas the alternative choice gives a more reasonable splitting of 14 cm^{-1}; cf. 11 cm^{-1} in $Mn_2(CO)_{10}$. A correlation of $\nu(CO)$ data for $Re_2(CO)_{10}$ and $Re(CO)_5I$

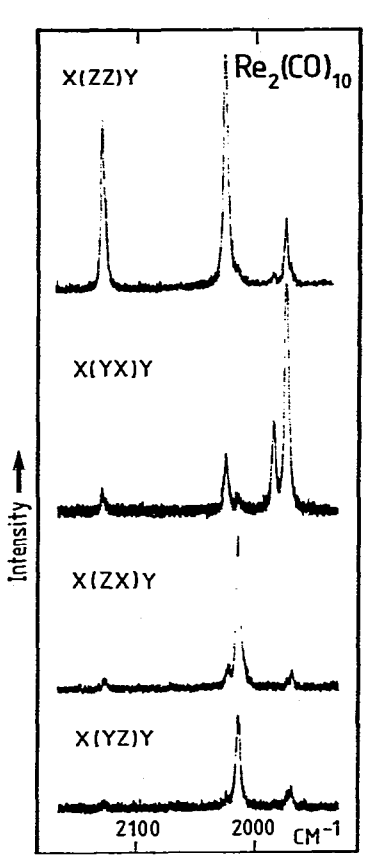

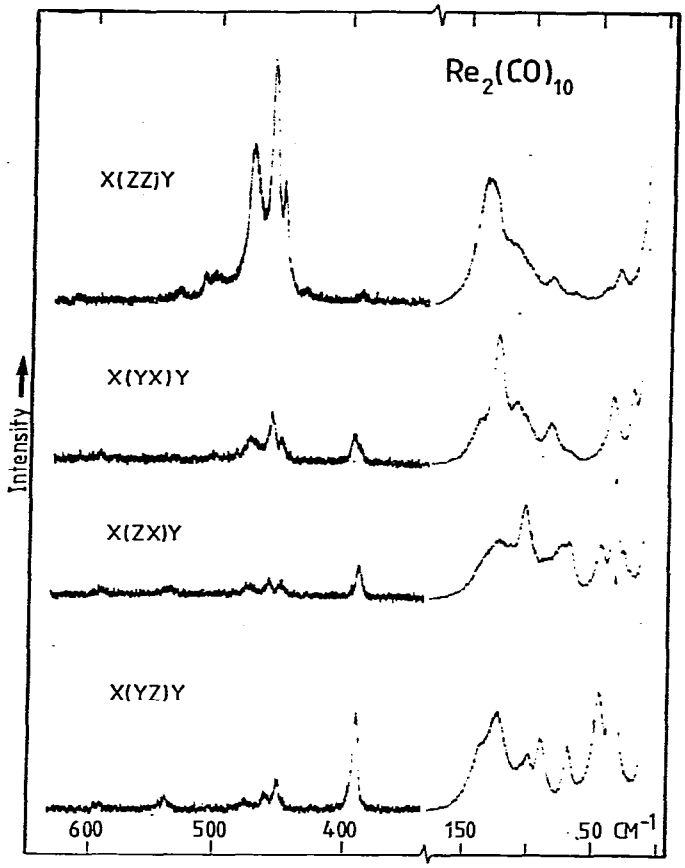

Fig. 2. Single-crystal Raman spectra of $Re_2(CO)_{10}$ at ambient temperature in the ν(CO) region, ca. 35 mW 632.8 nm excitation at the sample. Spectral slit width 2 cm^{-1}. The photomultiplier was run at 1000 V.

Fig. 3. Single-crystal Raman spectra of $Re_2(CO)_{10}$ in (a) the ReCO deformation and ν(Re—CO) region and, (b) the very-low-frequency region. Conditions as for Fig. 2, except that the PM voltage was 925 V for (b).

is shown in Table 5 and is seen to be fully consistent with that for equivalent manganese compounds.

The ν(Re—CO) and ReCO deformation region, 350—650 cm^{-1}

Earlier Raman solution work [2,21] led to identification of the three a_1 modes expected in this region, viz., 458, 475 and 614 cm^{-1}, all being polarised. The analogous bands in the solid are all unequivocally A_g in type, confirming the assignment to a_1 species.

All remaining bands must originate in molecular e_2 and e_3 species; a distinction is possible on the basis of intensity in the (ZZ) spectrum since e_3 modes should yield (ideally) zero intensity therein, whereas e_2 modes will not be zero. Further, from the correlation diagram of Table 2, both types of e species are expected to yield A_g/B_g doublets.

The 389/394 cm^{-1} pair are plainly of e_3 origin on these criteria and originate

TABLE 5

CORRELATION OF ν(CO) DATA (WAVENUMBERS (cm^{-1})) FOR $M_2(CO)_{10}$ AND $M(CO)_5X$ SPECIES, (M = Mn, Re)

$Mn(CO)_5Br$ [a]	C_{4v}	D_{4d}	$Mn_2(CO)_{10}$ [b]	$\Delta\nu(1)$ (cm^{-1}) [c]	$\Delta\nu(2)$ (cm^{-1}) [e]
2137.9		a_1, ν_1	2115.0		
	a_1 (equatorial)	b_2, ν_{11}	2045.8	57.5	69.2
2085.4	b_1	e_2, ν_{25}	2023.0	62.4	—
		e_1, ν_{17}	2014.7		
2052.2	e			54.1	33.2
		e_3, ν_{31}	1981.5		
		a_1, ν_2	1997.5		
2007.3	a_1 (axial)	b_2, ν_{12}	1983.8	16.7	13.7
$Re(CO)_5I$ [d]			$Re_2(CO)_{10}$ [b]		
		a_1, ν_1	2127.0		
2150	a_1 (equatorial)	b_2, ν_{11}	2070.4	51.3	56.6
2089	b_1	e_2, ν_{25}	2028.0	61.0	—
		e_1, ν_{17}	2014.0		
2048	e			49.0	30.0
		e_3, ν_{31}	1984.0		
		a_1, ν_2	1993.0		
1992	a_1 (axial)	b_2, ν_{12}	1997.3	—3.1	—4.3

[a] Data refer to CH_2Cl_2 solutions [11]. [b] Data from ref. 4. [c] Difference between value for the pentacarbonyl halide and the average of the correlating modes in $M_2(CO)_{10}$. [d] Data from ref. 21, $CHCl_3$ solution. [e] Difference between correlation doublets arising from a single C_{4v} mode.

in molecular ν_{35}, ν(Re—CO). Similarly, the prominent band at 451 cm^{-1} is of e_2 origin and shows no A_g/B_g splitting. There are two further e_2 modes at 503 and 513 cm^{-1}, ν_{26} and ν_{27}, both being ReCO deformations. This completes identification of the three allowed e_2 modes. It might be argued that these are a correlation doublet rather than two distinct e_2 modes as claimed. However, we note that this would give these weak bands the greatest correlation splitting of any mode in this region of the spectrum. Moreover, the final assignment reveals that correlation splitting is consistently weaker for e_2 than for e_3 modes, including the ν(CO) region.

It remains to locate the three ReCO deformation modes of e_3 type, ν_{32} to ν_{34}. One is certainly attributed to the 592/593 cm^{-1} doublet and a second to that at 534/539 cm^{-1} despite the presence of a weak (ZZ) component. The third is apparently absent. Additional weak features at 422 and 434 cm^{-1} cannot reasonably be attributed to this missing e_3 mode as this would upset the general separation which places all ν(M—CO) modes at lower frequency than MCO deformations. The 434 cm^{-1} band is most probably a factor group component of the IR-active band, present at this frequency in both solution and solid [21]; since it is of A_g type it cannot originate in a b_2 mode as proposed by Hyams, Jones et al. [21] but must be of e_1 species, ν_{21}. The extremely weak band at 422 cm^{-1} may not be fundamental. Finally, we note that all the ReCO deformation modes are weak in comparison with the ν(Re—CO) modes.

The region <200 cm^{-1}

In this region are expected δ(CReC) and other skeletal deformations, ν(Re–Re), and the lattice modes.

Two polarised bands were located in solution [2,21] at 103 and 125 cm^{-1}, corresponding to ν_6 and ν_7. The A_g band at 107 cm^{-1} is undoubtedly to be associated with ν_7, but it is not immediately clear whether the 129 or 122 cm^{-1} band is the equivalent of ν_6; it cannot be both as only one component is allowed. The 122 cm^{-1} band (A_g) has a close-lying B_g component, suggesting e_3 origin, whereas the 129 cm^{-1} band appears without a B_g component. The higher band is therefore attributed to ν_6. The question then arises as to which band corresponds to ν(Re—Re) and which to δ(CReC), although the usual caveat must be entered to the effect that there will be substantial mixing between the two types of internal coordinate.

In $Mn_2(CO)_{10}$ ν(Mn—Mn) is at 160 cm^{-1} [2]. Treating these molecules as pseudo-diatomics with the same force constant leads to a value of 125 cm^{-1} for ν(Re—Re). However, only a slight reduction in M—M force constant from M = Mn to M = Re would be enough to yield ν(Re—Re) at 107 cm^{-1}. Hyams, Jones and Lippincott [21] settled for the lower of the two possible assignments, chiefly because $Re(CO)_5I$ has a δ(CReC) mode at 130 cm^{-1}, although earlier workers had opted for the higher choice [25,26]. Moreover, the Re—Re bond polarisability values derived from Raman intensity measurements of both the 103 and 125 cm^{-1} bands also support the higher choice for ν(Re—Re) [9]. We note that high Raman intensity is not invariably associted with metal—metal stretching modes [10].

Our single-crystal measurements show that the 107 and 129 cm^{-1} bands have different intensity ratios between the (ZZ) and (YX) tensor components. The 107 cm^{-1} band has $I(YX) > I(ZZ)$, as does the 1976 cm^{-1} A_g ν(CO) mode, which is known to be axial in type. This is, moreover, the behaviour predicted on the basis of the oriented gas model, as shown above. The highly polarisable Re—Re bond lies along the molecular z-axis in D_{4d} and will have a large (zz) tensor component value (b), whereas the polarisability transverse to the bond (a) will be much smaller. Upon re-orientation of the tensor to crystallographic axes, the high intensity from b is thrown into the $(XY) \equiv (YX)(A_g)$ spectra, not the (ZZ) (A_g) one. Since the 129 cm^{-1} band has very high (ZZ) and zero (YX) intensity, we prefer the lower choice for ν(Re—Re). We believe that neither our own arguments, nor those of earlier workers, are unequivocal, and the truth may well be that there is so much coordinate mixing that the question is nonsensical. A normal-coordinate analysis and potential energy distribution calculation on the basis of our new assignment could well settle the question. Although we think it unlikely, it might also be argued that the 122 cm^{-1} band is ν(Re—Re) as it has the correct intensity behaviour.

We now consider assignment of the remaining low-frequency bands. The group of bands below 60 cm^{-1} is most reasonably attributed to lattice modes; the lowest three (18, 23, 30 cm^{-1}) are probably translational in type and include the predicted $A_g + 2B_g$ labels. The libratory lattice modes originate in molecular movements governed principally by the relative values of the moments of inertia (I). For $Re_2(CO)_{10}$, $I_x = I_y$ by symmetry, and $I_z \ll I_x$. Therefore the mode involving libration about the z-axis, $\nu(R_z)$, will be highest

TABLE 6

COMPARISON OF RAMAN-ACTIVE MODES FOR $M_2(CO)_{10}$, (M = Mn, Re)

		M = Re	M = Mn [c]				
A_1	ν_3	613	540	E_3	ν_{32}	593.5 [a]	673
	ν_4	476	480		ν_{33}	537.5 [a]	651
	ν_5	459.5	411		ν_{34}	n.o.	644
	ν_6	129	160 [b]		ν_{35}	391.5 [a]	465
	ν_7	107 [b]	116		ν_{36}	120.5 [a]	130
					ν_{37}	100	100.5 [a]
E_2	ν_{26}	513	555		ν_{38}	64.5 [a]	92
	ν_{27}	505	480				
	ν_{28}	451	421				
	ν_{29}	134 [a]	139				
	ν_{30}	83 [a]	125				

[a] Average of A_g, B_g frequencies, see Table 4. [b] ν(M—M). [c] Data from ref. 2.

in frequency. It originates as a_2 in D_{4d} and must therefore yield a B_g mode in the crystal; accordingly it is identified with the 71 cm^{-1} band.

If we are correct in our lattice mode assignment, all remaining B_g components from 60 to 200 cm^{-1} should originate from molecular internal modes. The Raman-active (in D_{4d}) modes numbers 29, 30 (e_2); 36, 37, 38 (e_3) should yield five B_g bands, whereas 6 are found. This implies that an originally IR-active mode (either b_2 or e_1 is permitted by the correlation field) is showing through, as was observed in the ν(CO) region for the b_2 mode ν_{11}. Assuming that the weakest B_g mode has this origin, we select the band at 95 cm^{-1}, and are gratified to note that an IR band is present [21] at 98 cm^{-1}. The remaining B_g bands are then paired with close-lying A_g components and attributed to either e_2 or e_3 species on the basis of (ZZ) and (YX) intensity. The assignment is summarised in Table 6: within each species modes are numbered in descending order, but their descriptions in Table 1 are to be taken in most cases only as an indication of the major contributing internal coordinate set. In particular, no distinction can be made between ρ, δ and π(MCO) modes in the absence of potential energy distribution calculations, but assignment to the class of ReCO angle deformations is definite.

Comparison with $Re(CO)_5X$ and $Mn_2(CO)_{10}$

Comparison of the $Re_2(CO)_{10}$ and $Mn_2(CO)_{10}$ assignments shows that the ReCO deformation modes span a range of 108 cm^{-1} whereas for MnCO angles the value is 197 cm^{-1}. We consider that the physical interactions between the two $M(CO)_5$ moieties are responsible for this difference, being greater for the case of the smaller metal. A semi-quantitative measure of support for this conjecture arises from the energy differences ($\Delta\nu(2)$ in Table 5) between pairs of ν(CO) modes whose difference arises from interactions between the two ends of each molecule; whilst quantitative support is found in the beautiful analysis of ν(CO) data by Bor and Sbrignadello [4]. Thus, in their Table 8, all four force constants which describe CO—CO interactions across the metal atoms are greater for manganese than for rhenium. In contrast, the three constants for interaction within one $M(CO)_5$ set are less for manganese than for rhenium.

For the very low-frequency deformations (<140 cm^{-1}) all values are slightly lower for the heavier molecule as expected.

A detailed comparison with extant data for $Re(CO)_5I$ serves only to emphasise the need for a definitive study of this molecule. Although much more is known about $Mn(CO)_5Br$, even for it a number of key mode assignments are in doubt, notably that of ν_3 (645 cm^{-1}). In future definitive studies of the pentacarbonyl halides we believe that our assignments for $Mn_2(CO)_{10}$ and $Re_2(CO)_{10}$ will provide a useful point of reference and a check on consistency.

Acknowledgement

We thank the S.R.C. for support.

References

1 E.O. Brimm, M.A. Lynch and W.J. Sesny, J. Amer. Chem. Soc., 76 (1954) 3831.
2 References to mid-1970 are given in: D.M. Adams, M.A. Hooper and A. Squire, J. Chem. Soc. (A), (1971) 71.
3 W.T. Wozniak and R.K. Sheline, J. Inorg. Nuclear Chem., 34 (1972) 3765.
4 G. Bor and G. Sbrignadello. J. Chem. Soc. Dalton, (1974) 440.
5 R.M. Wing and D.C. Crocker, Inorg. Chem., 6 (1967) 289.
6 D.M. Adams, M.A. Hooper and A. Squire, J. Chem. Soc. Chem. Comm., (1970) 1188.
7 D.N. Kariuki and S.F.A. Kettle, J. Organometal. Chem., 105 (1976) 209.
8 G.O. Evans, W.T. Wozniak and R.K. Sheline, Inorg. Chem., 9 (1970) 979.
9 C.O. Quicksall and T.G. Spiro, Inorg. Chem., 9 (1970) 1045.
10 B.I. Swanson, J.J. Rafalko, D.F. Shriver, J. SanFilippo and T.G. Spiro, Inorg. Chem., 14 (1975) 1737.
11 D.K. Otteson, H.B. Gray, L.H. Jones and M. Goldblatt, Inorg. Chem., 12 (1973) 1051.
12 I.S. Butler and C.F. Shaw, J. Raman Spectroscopy, 2 (1974) 257.
13 D.M. Adams and A. Squire, J. Chem. Soc. A, (1968) 2817.
14 V. Valenti, F. Cariati, C. Forese and G. Zerbi, Inorg. Nucl. Chem. Lett., 3 (1967) 237.
15 D.N. Kariuki and S.F.A. Kettle, Inorg. Chem., 17 (1978) 1018.
16 R.J.H. Clark and B.C. Crosse, J. Chem. Soc. A, (1969) 224.
17 W.F. Edgell, J.W. Fisher, G. Asato and W.M. Risen, Inorg. Chem., 8 (1969) 1103.
18 A. Davison and J.W. Faller, Inorg. Chem., 6 (1967) 845.
19 I.S. Butler and H.K. Spendjian, Canad. J. Chem., 47 (1969) 4117.
20 I.J. Hyams and E.R. Lippincott, Spectrochim. Acta, A, 25 (1969) 1845.
21 I.J. Hyams, D. Jones and E.R. Lippincott, J. Chem. Soc. A, (1967) 1987.
22 W.A. McAllister and A.L. Marston, Spectrochim. Acta A, 27 (1971) 523.
23 L.F. Dahl and R.E. Rundle, Acta Cryst., 16 (1963) 419.
24 M.A. Hooper and D.R. Russell, unpublished work.
25 J. Lewis, A.A. Manning, J.R. Miller, M.J. Ware and F. Nyman, Nature (London), 207 (1965) 142.
26 F.A. Cotton and R.M. Wing, Inorg. Chem., 4 (1965) 1328.